

# A Numerical Prediction Model for Vibration and Noise of Axial Flux Motors

Sunghyuk Park, Wonho Kim, and Sung-II Kim, *Member, IEEE*

**Abstract**—A numerical procedure to predict vibration and acoustic noise due to electromagnetic excitation forces in an axial flux motor (AFM) is presented and applied to a motor with ferrite magnets for electric vehicles. The methodology includes the calculation of radial magnetic forces exerted on stator inner surfaces using electromagnetic solver to account for vibration and noise of the motor. Fundamental and high-order harmonics of the magnetic forces are then obtained via fast Fourier transform process. Structural analyses such as modal and harmonic analysis are conducted to investigate natural resonant frequencies of the motor system and modal shapes highly responsible for vibration of the frame and acoustic noise. Magnitudes of vibration displacement on the motor housing surface and sound pressure level at a given point in the space are predicted using harmonic and acoustic analyses, respectively. Motor performance tests were conducted to validate the model, and the results showed that the model predictions agree well with the observations from the experiments.

**Index Terms**—Acoustic noise, axial flux motor (AFM), electromagnetic stress, noise measurement, numerical prediction, structural dynamics, vibration.

## I. INTRODUCTION

**I**N ORDER to ensure driving comfort, a great effort to reduce levels of vibration and acoustic noise of traction motors for electric vehicles has been made for the last couple of decades. However, vibration and acoustic noise are still crucial problems of traction motors particularly due to excitation forces with high-order harmonics.

Several sources have been identified as contributing to vibration and noise of electric motors through extensive experimentation. First, a fault in mechanical assembly such as interaction between bearing and a rotor shaft can produce vibration and noise [1]–[4]. Second, ventilating air flowing through an electric motor can generate aerodynamic vibration and noise [5]–[7]. Vibration is also generated from a flawed coupling between an electric machine and a load such as misaligned shafts, belts, gear, and so on [2], [4], [8], [9]. The mount of a motor to a foundation or other structures is also a crucial factor for vibration and acoustic noise [2], [10], [11]. Finally, electromagnetic sources due to magnetic stresses with high-order time and spatial harmonics, eccentricity, and rotor unbalance

have been recognized to have the most significant effect on the vibration and thus acoustic noise of electric motors [2], [12]–[15].

To avoid time-consuming and instrumentation-intensive experiments, a considerable amount of research has been done in order to understand the mechanisms of vibration and acoustic noise by using numerical modeling methodology [14], [16]–[20]. However, these studies have a couple of limitation. First, geometry of an electric motor system has been considered as a two-dimension plane in both electromagnetic and structural numerical analyses [18], [20]. This two-dimensional (2-D) assumption has worked well and its results agree very well with the experimental data in an electromagnetic analysis. However, structural and acoustic behaviors such as natural frequencies of the motor system and distribution of sound pressure depend highly on its three-dimensional (3-D) shape and constraint conditions [21], [22]. In addition, axial flux motors cannot be assumed to be a 2-D model. Recently, acoustic noise and vibration of axial flux motors have been predicted using finite element method [23], [24]. Second, these studies have neglected high-order harmonic force components of electromagnetic stresses, while both of the fundamental and high-order time harmonics at the same time excite stator inner surfaces [16]. To overcome the aforementioned problems, this paper presents a procedure for predicting vibration and acoustic noise due to electromagnetic stresses of axial flux motors with both fundamental and high-order time harmonics by incorporating a variety of numerical methodologies into a single 3-D multiphysical numerical procedure.

The outline of this paper is as follows. First, to facilitate the development of vibration and acoustic noise prediction model, Maxwell stress tensor method and decomposition of forces based on harmonic frequencies were briefly reviewed for calculating radial and tangential magnetic forces on stator tooth surfaces. Modal and harmonic structural analyses were conducted to investigate the vibration behavior of the motor system. An acoustic noise prediction model was then developed by incorporating an acoustic indirect boundary element solver and used to predict sound pressure level at an arbitrary point in the space. Finally, the prediction model was validated by comparing the actual noise measurement results with the model prediction.

## II. MODEL DEVELOPMENT

### A. Specification of Motor

Recently, the authors of [25] designed an axial flux ferrite magnet motor with a novel rotor configuration and verified its

Manuscript received April 1, 2013; revised September 15, 2013 and December 2, 2013; accepted December 4, 2013. Date of publication January 14, 2014; date of current version May 2, 2014.

The authors are with the Compressor and Motor Business Team, Digital Appliances, Samsung Electronics, Suwon 442-742, Korea (e-mail: sunghyuk1.park@samsung.com).

Color versions of one or more of the figures in this paper are available online at <http://ieeexplore.ieee.org>.

Digital Object Identifier 10.1109/TIE.2014.2300034

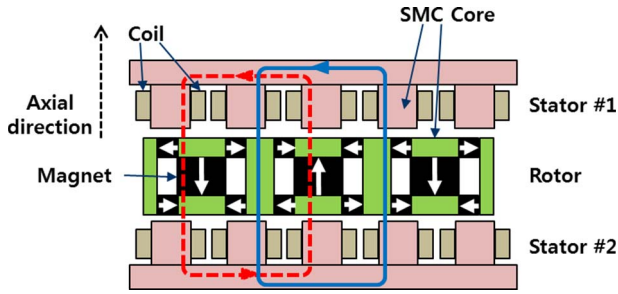


Fig. 1. Schematic illustration of an axial flux type motor and its d-(dashed) and q-axis (solid) paths [25].

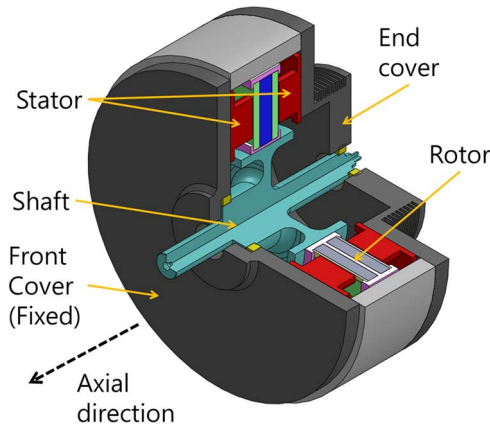


Fig. 2. Exploded view of 3-D model of the motor.

TABLE I  
SUMMARY OF DIMENSION AND SPECIFICATION OF THE MOTOR [25]

Items	Value (Unit)
Outer diameter	302 mm
Stack length	90 mm
Air-gap	1 mm
Permanent magnet (PM)	Ferrite (NMF-12G)
Remnant flux density of PM	0.45 T
DC link voltage	120 V (at peak) 144 V (at rated)
Max. (peak) / Rated power (continuous)	18.3 / 7.75 kW
Max. (peak) / Rated current (continuous)	240 / 70 Arms
Base / Max. speed	2500 / 7000 rpm (at peak) 4000 / 7000 rpm (at rated)
Number of poles / slots	10 / 24

performance. Fig. 1 shows its configuration of the rotor and stator with arrows indicating the magnetization directions of ferrite magnets. Fig. 2 presents an exploded view of a 3-D model of the prototype motor. Table I lists summarized specification of the axial flux type motor studied in this prediction and validation process. It was observed that the torque value of the prototype motor was high since bisecting a magnet into two pieces creates an additional q-axis path, leading to efficiently using reluctance torque component [25]. More detailed specification and dimensions of the motor are listed in [25].

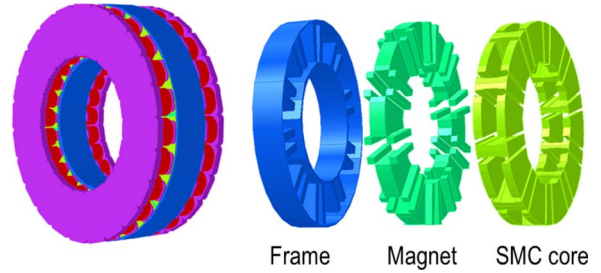


Fig. 3. Three-dimensional model of the prototype motor.

### B. Prediction Procedure Overview

The numerical procedure presented in this paper predicts vibration and acoustic noise behaviors of electric motors over a wide range of operation conditions. The model combines an electromagnetic and structural analysis together with an acoustic boundary element solver. First, electromagnetic forces both in the axial direction and the direction parallel to a tooth surface are calculated by integrating motor geometry, material properties, and operating. Modal and harmonic analyses are then conducted to obtain natural resonant frequencies and corresponding modal shapes of the motor system. Excitation forces in the frequency domain are then applied on the slot tooth surface to calculate vibration of the motor outer surfaces. Finally, acoustic noise due to the vibrating motor is predicted as sound pressure level at a given distance from the motor.

This research has focused on vibration and noise generated due to electromagnetic sources and assumed no rotor eccentricity and rotor unbalance. Mechanical and aerodynamic vibration and noise sources were also neglected.

### C. Electromagnetic Analysis

Electromagnetic pressure on the slot tooth surfaces was calculated using a 3-D electromagnetic solver, Opera3D. Fig. 3 presents components of a 3-D model of the axial flux type motor studied in this work.

Magnitudes of electromagnetic pressures generated along the air gap between the rotor and stator were calculated using Maxwell stress tensor method [26]

$$\sigma_{ij} = \frac{1}{\mu_0} B_i B_j - \frac{1}{2\mu_0} B^2 \delta_{ij} \quad (1)$$

where  $\sigma_{ij}$  is a stress due to electromagnetic field,  $\mu_0$  is the permeability of vacuum,  $B_i$  and  $B_j$  are  $i$ th and  $j$ th components of the magnetic flux density in the air gap, relatively, and  $B$  is its magnitude. Resultant forces applied on each tooth surface were then obtained by multiplying the area of each tooth surface.

Fig. 4 shows an axial stress on the surface of slot 1 rotating at the speed of 4000 rpm. Such forces were then decomposed by fast Fourier transform (FFT) into a frequency domain in order to account for the effect of high-order harmonic components on vibration and noise behavior of the motor (Fig. 5). The force components expressed in the frequency domain were then translated into structural and acoustic analyses. It was observed that these stresses fluctuate over time at a frequency of 667 Hz, twice as high as the motor line input frequency, 333 Hz. In

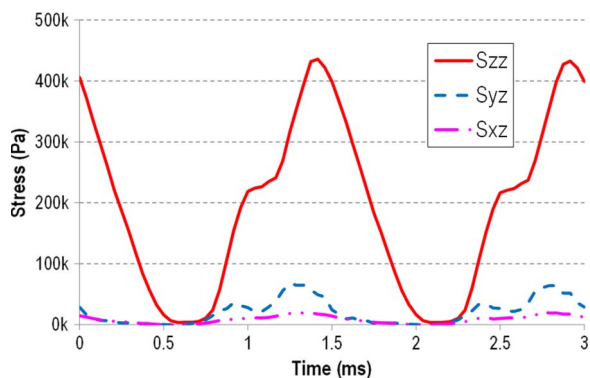


Fig. 4. Axial stress on slot #1 at 4000 rpm.

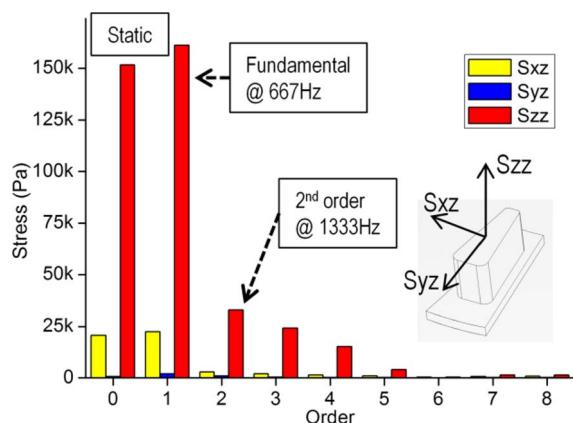


Fig. 5. FFT decomposition result of axial excitation force on slot #10 at 4000 rpm.

addition, the magnitude of the axial stress,  $S_{zz}$ , was observed to be significantly higher than the other stress components,  $S_{xz}$  and  $S_{yz}$ . As a result, the effect of such shear stress components on structural vibration and acoustic noise were neglected in this study.

*D. Structural Analysis*

Amplitudes of displacement and acceleration on the motor frame surface increase as either of fundamental or any high-order harmonic components of the excitation forces approaches close to any of natural frequencies of the motor system. Mechanical resonance occurs when the frequency is equal to any of natural frequencies.

It has been known in conventional radial-type motor that low even-number circumferential modes on frame have a significant effect on the airborne noise generation, while its axial vibration is negligible. This is because magnetic forces are applied on slot tooth surfaces covered with its cylindrical frame. In axial flux motors, however, electromagnetic excitation forces are applied on slot tooth surfaces in the axial direction. Vibration thus generated is mainly transmitted to front and back covers on which the stators are attached. This indicates that in axial flux type motors vibration on the front and rear motor covers is significant rather than on the surface along its circumference, possibly leading to high acoustic noise in the axial direction.

Modal and harmonic analyses were conducted by structural analysis solver, ANSYS. Natural frequencies and vibration be-

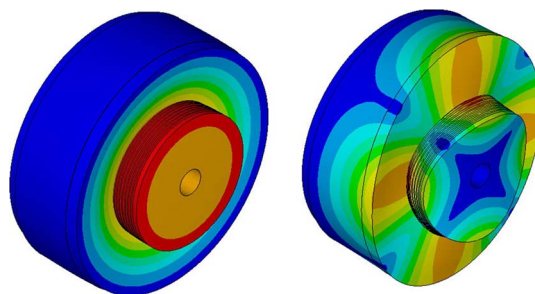


Fig. 6. Modal shapes at natural frequencies of 1299 Hz (left) and 3078 Hz (right).

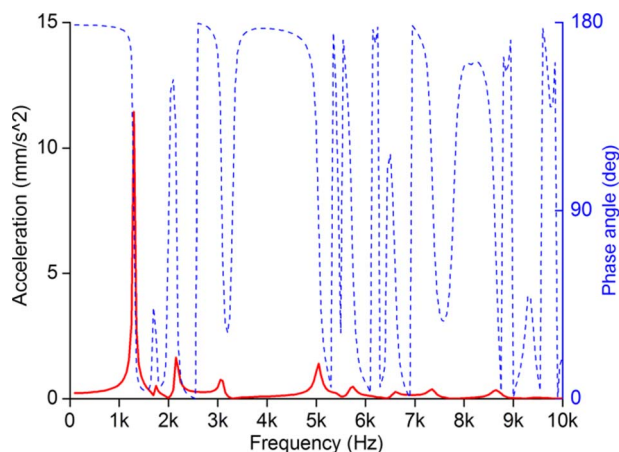


Fig. 7. Numerically predicted acceleration amplitude on the motor frame surface and corresponding phase angle over a range of frequency.

havior of a motor system significantly depend on the mounting condition of the motor to a foundation or other structure. In order to reflect the actual constraint conditions of the motor system, the front cover was assumed to be fully constrained to the test jig. First two natural frequencies for axial vibration and corresponding mode shapes obtained by ANSYS are presented in Fig. 6. The axial flux motor system resonates as a frequency of excitation force components moves close to any of its axial resonant frequencies.

In order to investigate how the motor system responds to an excitation force with various frequencies, a harmonic analysis was conducted with a one newton (1N) unit force on a slot tooth surface in an axial direction, and a magnitude of acceleration at a point located on the motor front cover surface was calculated over a range of force frequencies using ANSYS. The amplitude of axial acceleration on the motor back cover and corresponding phase angle is presented in Fig. 7, and it was predicted that the first mechanical resonance is the most crucial and occurs at 1299 Hz.

*E. Acoustic Analysis*

Electromagnetic forces applied on the stator tooth surfaces with both fundamental and high-order harmonic components and natural frequencies with corresponding modal shapes were incorporated into an acoustic boundary element solver, LMS Virtual.Lab Acoustic to predict acoustic noise of the axial flux type motor. As mentioned in the previous section, it has been

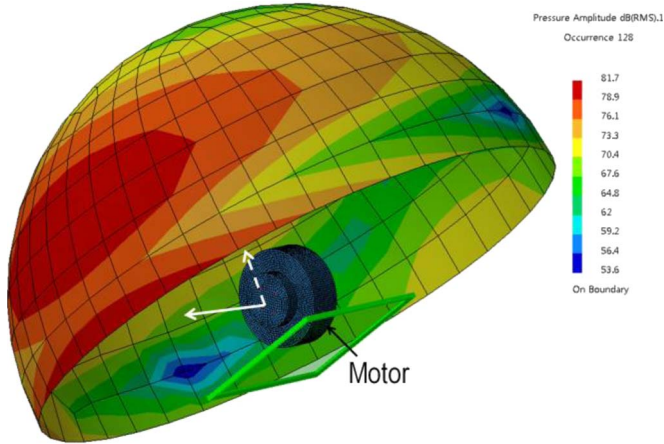


Fig. 8. Sound pressure distribution at 1300 Hz rotating at 6000 rpm on the surface with 1-m radius from the motor center. Solid and dashed arrows indicate axial and radial directions, respectively.

assumed in this paper that vibration due to electromagnetic excitation forces is the most dominant factor of the airborne noise, and other noise sources such as mechanical, aerodynamic, and other sources from load couplings were neglected.

Sound pressure,  $p$ , at a given point in the space was calculated by using

$$p(\omega) = \{ATV(\omega)\}^T \{v_b(\omega)\} \quad (2)$$

where  $ATV$  is an acoustic transfer vector,  $\omega$  is an angular velocity of a specific frequency with the range of interest, and  $v_b$  is structural velocities on the motor frame surface. The normal boundary velocities were obtained by using the results from the modal analysis in the previous section

$$\{v_b(\omega)\} = i\omega[\Phi_n] \{MRSP(\omega)\} \quad (3)$$

where  $\Phi_n$  is a matrix of the modal vectors,  $MRSP$  is a modal response vector of the motor structure at a given frequency. The sound pressure level at an arbitrary point in the space and frequency was then calculated as in

$$p(\omega) = i\omega \{ATV(\omega)\}^T [\Phi_n] \{MRSP(\omega)\}. \quad (4)$$

More details of the derivation and calculation methodology are described in [27].

The distribution of sound pressure at a frequency of 1300 Hz at a motor speed of 6000 rpm on the surface with 1-m diameter from the center of the motor is presented in Fig. 8. It was noted that unlike conventional radial type motors the magnitude of sound pressure along the circumferential surface of the motor is lower than one in the axial direction. This is so because shear components of electromagnetic excitation forces have been neglected as mentioned in the previous section and the two stators were attached to both front and back covers in the axial direction as shown in Fig. 2, leading to no significant radial vibration of the motor frame. In addition, the magnitude is high on the surface from the back cover than the front cover because the vibration of the motor surface was predicted under the boundary condition such that the front side of the motor was fixed to the test jig.

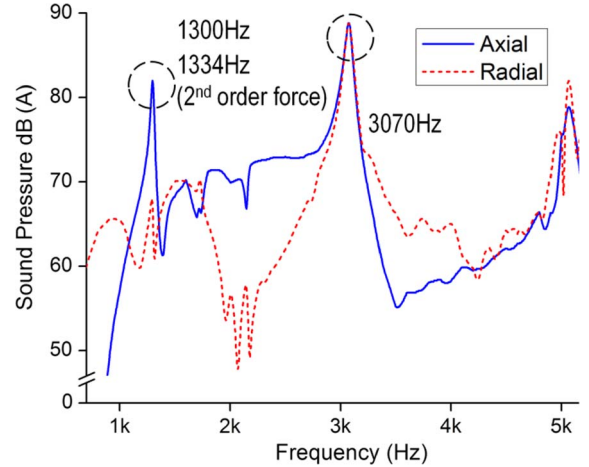


Fig. 9. Sound pressure level prediction results at the points 1 m from the center of the motor in axial (solid) and radial (dashed) directions at 6000 rpm.

Fig. 9 presents the FFT results of predicted sound pressure levels at the points 1 m from the center of the motor in axial and radial directions. The motor was set to operate at its maximum power condition at a speed of 6000 rpm. At 3100 Hz, sound pressure levels at both directions were predicted to be approximately 88.8 dB(A). This can be explained by the result that the axial modal shape is predicted at 1299 Hz, while both the back cover and cylindrical frame of the motor vibrate in both axial and radial directions at 3078 Hz as shown in Fig. 6. It was predicted that the amplitudes of sound pressure levels are higher at the location of axial direction than radial direction over a range of frequency, which indicates the vibration behavior in the axial direction have more significant effect than in the radial direction on acoustic noise in axial flux motors.

### III. MODEL VALIDATION

To determine the effectiveness of using the model to predict vibration and acoustic noise of axial flux type electric motors, vibration and noise were measured at the same operating conditions and motor configurations used for the numerical simulations to compare the experimental results with the results from the model predictions.

#### A. Experimental Setup

The actual picture of the axial flux ferrite magnet motor and the vibration measurement points is shown in Fig. 10. Acceleration values in three axes were measured at the points on the back cover and on radial frame surface of the motor using B&K type 4520 triaxial accelerometer and FFT analyzer system as indicated with arrows in Fig. 10. Each measurement was replicated three times for given operating conditions.

#### B. Results and Discussion

Acceleration levels were measured from 1000 to 6000 rpm at the maximum power region of the motor and the measurement data of the axial acceleration on the motor back cover was shown as a waterfall plot in Fig. 11. The fundamental frequency

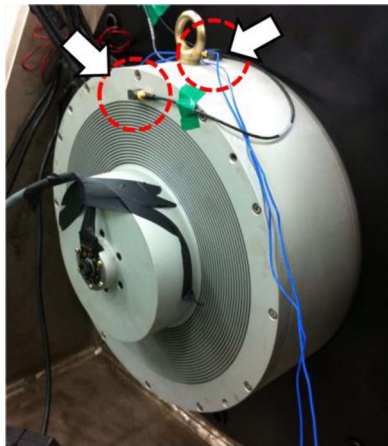


Fig. 10. Actual motor set fixed to the dynamometer and accelerometers for measurement indicated with arrows.

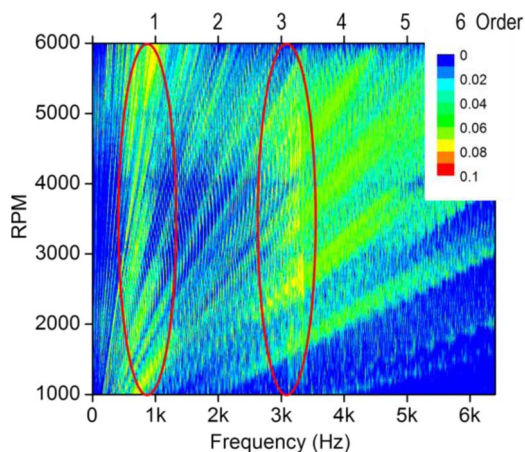


Fig. 11. Waterfall plot of axial acceleration amplitudes.

of electromagnetic stresses of 10-pole motors is two times as high as its electric frequency. It was observed that magnitudes of acceleration due to fundamental and harmonic components of electromagnetic excitation forces are much higher than those due to fundamental and harmonics of the rotor revolution speed. The magnitude of acceleration is observed to be high approximately at frequency ranges of 800 to 1000 Hz and 2900 to 3100 Hz for all rotating speed. This is because the motor system resonates at such frequencies as described in the structural analysis section. The difference between values of prediction and measurement in frequency may be due to the effect of additional mass and stiffness of winding and the contact property between the stators and the motor frame.

Sound pressure level was measured at the point 1 m from the center of the motor using B&K type 4191 free-field microphone and Audio Analyzer system. A-weight acoustic filter was applied to both experimental measurement data and prediction values. Each measurement was replicated three times for given operating conditions.

Sound pressure was measured during performance testing of the motor and not in an anechoic chamber. As a result, the measurement data contained not only the acoustic noise due to vibrating surface of the motor system but background noise

TABLE II  
SUMMARY OF SOUND PRESSURE LEVEL (SPL)  
MEASUREMENT AND MODEL PREDICTION

Motor speed (rpm)	Experimental result SPL (dB(A))	Model prediction SPL (dB(A))
1000	75	72.3
2000	87	89.1
3000	98	99.7
4000	105	102.5
5000	109	103.2
6000	114	107.6

from the test site and noise from the load motor of the test dynamometer. The noise level measured with the motor stopped was subtracted from each measured sound pressure level.

The overall measurement data of sound pressure level in the axial direction were listed in Table II. The prediction results until 4000 rpm were found to agree well with the experimental measurement within 3 dB, while the error between the prediction and experimental results is approximately 6 dB at speeds higher than 4000 rpm. This may be so because at higher speeds significant acoustic noise is generated not only from the test motor but also from the load motor. Further experiments need to be done with a dynamometer and load motor outside an anechoic chamber in order to improve the measurement accuracy and to eliminate the effect of the background noise.

#### IV. CONCLUSION

A numerical methodology for the prediction of vibration and acoustic noise of axial flux motors has been developed. The procedure developed is capable of predicting the amplitude of the surface displacement and distribution of sound pressure at an arbitrary point in the space due to both fundamental and high-order harmonics electromagnetic excitation forces exerted on the surfaces of stator teeth. The following specific conclusions can be made.

- 1) Electromagnetic forces were calculated by Maxwell stress tensor method using a 3-D electromagnetic solver. The force on each slot surface was then decomposed by FFT into fundamental and high-order harmonic force components with amplitudes and phase angles over a range of frequencies.
- 2) Modal and harmonic analyses were conducted to obtain natural frequencies and corresponding modal shapes of the motor frame. Axial vibration modes have a significant effect on vibration and airborne noise of axial flux motors.
- 3) Sound pressure level at a given point in the space was predicted using an indirect boundary element analysis solver by incorporating the effect of structural vibration behavior and the combination of fundamental and higher order harmonic forces.
- 4) The vibration and acoustic noise prediction methodology was validated by actual experiments over a range of motor speeds. The model successfully predicted the sound pressure within errors in 3 dB at low speeds and up to 6 dB at high speeds between the predictions and experiments.

## REFERENCES

- [1] K. N. Srinivas, "Static and dynamic vibration analyses of switched reluctance motors including bearings, housing, rotor dynamics, and applied loads," *IEEE Trans. Magn.*, vol. 40, no. 4, pp. 1911–1919, Jul. 2004.
- [2] J. F. Gieras, C. Wang, and J. C. Lai, *Noise of Polyphase Electric Motors*. Boca Raton, FL, USA: CRC Press, 2006.
- [3] F. Immovilli, M. Cocconcelli, A. Bellini, and R. Rubini, "Bearing fault model for induction motor with externally induced vibration," *IEEE Trans. Ind. Electron.*, vol. 60, no. 8, pp. 3408–3418, Aug. 2013.
- [4] S. Nandi, H. A. Toliyat, and X. Li, "Condition monitoring and fault diagnosis of electrical motors—A review," *IEEE Trans. Energy Convers.*, vol. 20, no. 4, pp. 719–729, Dec. 2005.
- [5] S. L. Nau and H. G. G. Mello, "Acoustic noise in induction motors: Causes and solutions," in *Conf. Rec. IAS Petroleum Chem. Ind. Conf.*, 2000, pp. 253–263.
- [6] J. O. Fiedler and K. A. Kasper, "Acoustic noise in switched reluctance drives: An aerodynamic problem?" in *Proc. IEEE Int. Conf. Elect. Mach. Drives*, 2005, pp. 1275–1280.
- [7] R. P. Lisner and P. L. Timar, "A new approach to electric motor acoustic noise standards and test procedures," *IEEE Trans. Energy Convers.*, vol. 14, no. 3, pp. 692–697, Sep. 1999.
- [8] D. H. Lee, J. H. Lee, and J. W. Ahn, "Mechanical vibration reduction control of two-mass permanent magnet synchronous motor using adaptive notch filter with fast Fourier transform analysis," *IET Elect. Power Appl.*, vol. 6, no. 7, pp. 455–461, Aug. 2012.
- [9] H. Heno, S. H. Kia, and G. Capolino, "Torsional-vibration assessment and gear-fault diagnosis in railway traction system," *IEEE Trans. Ind. Electron.*, vol. 58, no. 5, pp. 1707–1717, May 2011.
- [10] S. Kreitzer and J. Obermeyer, "The effects of structural and localized resonances on induction motor performance," *IEEE Trans. Ind. Appl.*, vol. 44, no. 5, pp. 1367–1375, Sep./Oct. 2008.
- [11] W. R. Finley, M. M. Hodowanec, and W. G. Holter, "An analytical approach to solving motor vibration problems," *IEEE Trans. Ind. Appl.*, vol. 36, no. 5, pp. 1467–1480, Sep./Oct. 2000.
- [12] S. A. Swann and S. A. Nasar, "Effect of rotor eccentricity on magnetic field in air gap of a non-salient-pole machine," *Proc. Inst. Elect. Eng.*, vol. 110, no. 5, pp. 903–915, Jul. 1964.
- [13] J. Krotzsch and B. Piepenbreier, "Radial forces in External rotor permanent magnet synchronous motors with non-overlapping windings," *IEEE Trans. Ind. Electron.*, vol. 59, no. 5, pp. 2267–2276, May 2012.
- [14] D. J. Kim, J. W. Jung, J. P. Hong, K. J. Kim, and C. J. Park, "A study on the design process of noise reduction in induction motors," *IEEE Trans. Magn.*, vol. 48, no. 11, pp. 4638–4641, Nov. 2012.
- [15] K. T. Kim, K. S. Kim, S. M. Hwang, T. J. Kim, and Y. H. Jung, "Comparison of magnetic forces for IPM and SPM motor with rotor eccentricity," *IEEE Trans. Magn.*, vol. 37, no. 5, pp. 3448–3451, Sep. 2001.
- [16] D. Kim, J. Kim, and J. Hong, "A study on the reduction of noise and vibration of SPM according to reduction of permanent magnet," in *Proc. Int. Conf. Elect. Mach. Syst.*, 2010, pp. 1252–1255.
- [17] T. Sun, J. Kim, G. Lee, and J. Hong, "Effect of pole and slot combination on noise and vibration in permanent magnet synchronous motor," *IEEE Trans. Magn.*, vol. 47, no. 5, pp. 1038–1041, May 2011.
- [18] G. He, Z. Huang, and D. Chen, "Two-dimensional field analysis on electromagnetic vibration-and-noise sources in permanent-magnet direct current commutator motors," *IEEE Trans. Magn.*, vol. 47, no. 4, pp. 787–794, Apr. 2011.
- [19] G. He, Z. Huang, R. Qin, and D. Chen, "Numerical prediction of electromagnetic vibration and noise of permanent-magnet direct current commutator motors with rotor eccentricities and glue effects," *IEEE Trans. Magn.*, vol. 48, no. 5, pp. 1924–1931, May 2011.
- [20] J. W. Jung, S. H. Lee, G. H. Lee, J. P. Hong, D. H. Lee, and K. N. Kim, "Reduction design of vibration and noise in IPMSM type integrated starter and generator for HEV," *IEEE Trans. Magn.*, vol. 46, no. 6, pp. 2454–2457, Jun. 2010.
- [21] J. J. Radice, "On the effect of local boundary condition details on the natural frequencies of simply-supported beams: Eccentric pin supports," *Mech. Res. Commun.*, vol. 39, no. 1, pp. 1–8, Jan. 2012.
- [22] M. A. Nasser, "Modal based predictive design and analysis of electric motors," in *Proc. Conf. 22th IMAC, Conf. Expo. Struct. Dyn.*, 2004, pp. 1–22.
- [23] Q. Li and Y. Wnag, "The analysis of finite element for the noise of axial flux surface mounted permanent magnet synchronous machines' system," in *Proc. Int. Conf. E-Product E-Service E-Entertainment*, 2010, pp. 1–4.
- [24] Z. Song, R. Tang, S. Yu, and H. Zhang, "The influence of vibration and acoustic noise of axial flux permanent magnet machines by inverter," in *Proc. Int. Conf. Mech. Autom. Control Eng.*, 2010, pp. 2423–2426.
- [25] W. Kim and S. Park, "Novel ferrite magnet motors for in-wheel type EVs," *IEEE Trans. Magn.*, submitted for publication.
- [26] M. Marinescu and N. Marinescu, "Numerical computation of torques in permanent magnet motors by Maxwell stresses and energy method," *IEEE Trans. Magn.*, vol. 24, no. 1, pp. 463–466, Jan. 1988.
- [27] O. von Estorff, *Boundary Elements in Acoustics: Advances and Application*. Southampton, U.K.: WIT Press, 2000.



**Sunghyuk Park** received the B.S and M.S. in mechanical design and production engineering from Seoul National University, Seoul, Korea, in 1998 and 2000, respectively, and the Ph.D. degree in mechanical engineering from the University of Illinois at Urbana-Champaign, Champaign, in 2007.

Currently, he is a Senior Engineer with the Compressor and Motor Business Team, Digital Appliances, Samsung Electronics, Suwon, Korea. He is responsible for analyzing the structural robustness of electric motors and their vibration and acoustic noise. During his academic and industrial career, he has worked on developing various numerical models, including developing cutting force prediction models, designing ring-type ultrasonic motors, and predicting tactile sensation with haptic devices using electrorheological fluid.



**Wonho Kim** received the B.S., M.S., and Ph.D. degrees in electrical engineering from Hanyang University, Seoul, Korea in 2005, 2007, and 2011, respectively.

Currently, he is a Senior Engineer with the Compressor and Motor Business Team, Digital Appliances, Samsung Electronics, Suwon, Korea. His research interests include motor design, analysis of motors and generators, and applications of motor drives, such as electric vehicles and home appliances.



**Sung-II Kim** (S'07–M'13) received the B.S. and M.S. degrees in electrical engineering from Changwon National University, Changwon, Korea, in 2003 and 2005, respectively, and the Ph.D. degree in automotive engineering from Hanyang University, Seoul, Korea, in 2011.

Currently, he is a Senior Engineer with the Compressor and Motor Business Team, Digital Appliances, Samsung Electronics, Suwon, Korea. He is responsible for developing compressor motors with ferrite magnets for system air conditioners.